Electronic Supplementary Material (ESI) for Dalton Transactions.

Electronic Supplementary Information

Syntheses, structures and magnetic properties of macrocyclic Schiff base-supported homodinuclear lanthanide complexes†

Feng Gao,*[a] Yi-Quan Zhang,*[b] Wang Sun,[a] Huan Liu,[a] and Xiaoyu Chen*[c]

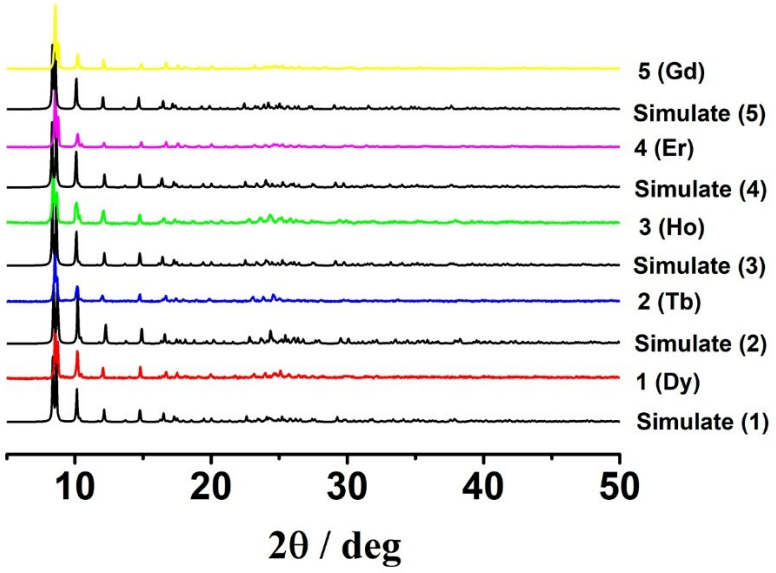

Fig. S1 Experimental and simulated PXRD patterns of complexes **1**–**5**.

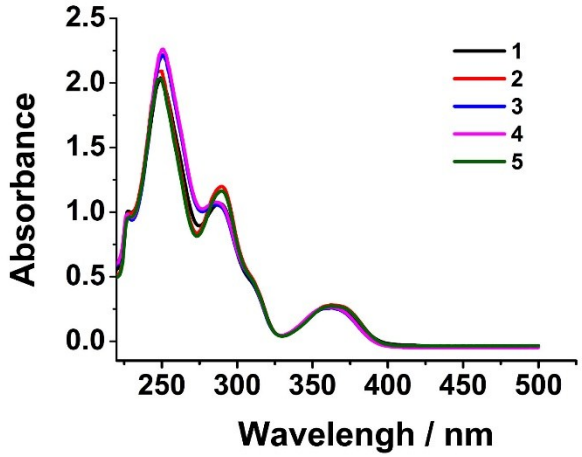

Fig. S2 UV-Vis absorption spectra for complexes **1**–**5** in dichloromethane (c = 6 × 10^{-6} M).

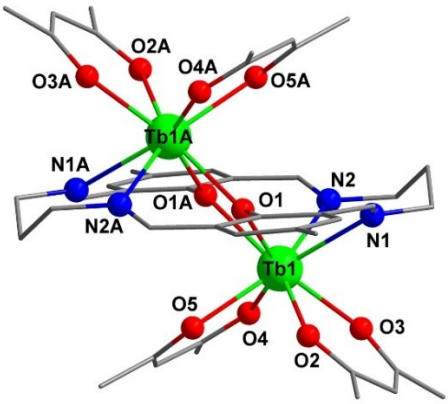

Fig. S3 Molecular structure of complex **2** with hydrogen atoms and solvent molecules omitted for clarity.

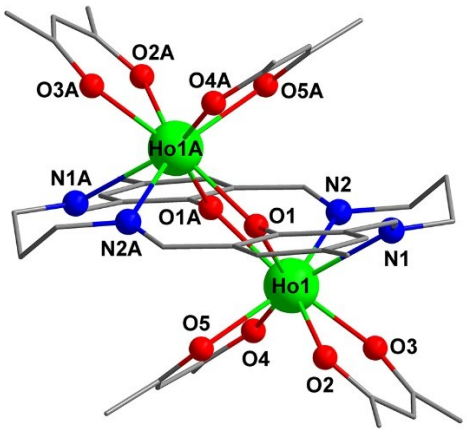

Fig. S4 Molecular structure of complex **3** with hydrogen atoms omitted for clarity.

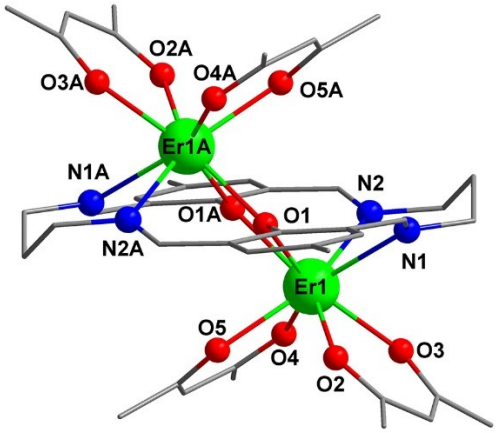

Fig. S5 Molecular structure of complex **4** with hydrogen atoms omitted for clarity.

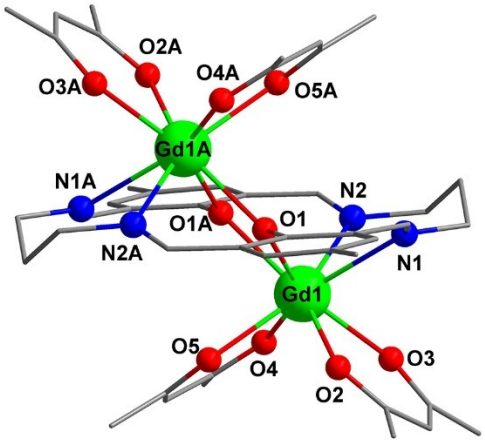

Fig. S6 Molecular structure of complex **5** with hydrogen atoms omitted for clarity.

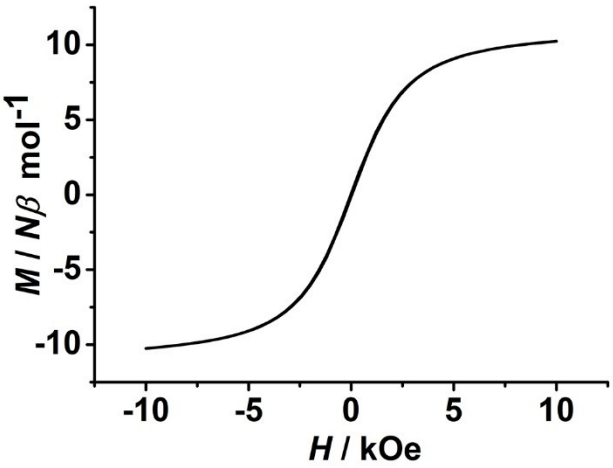

Fig. S7 Hysteresis loop for complex **1** at 2.0 K with a sweeping rate of 100 Oe s^{-1}.

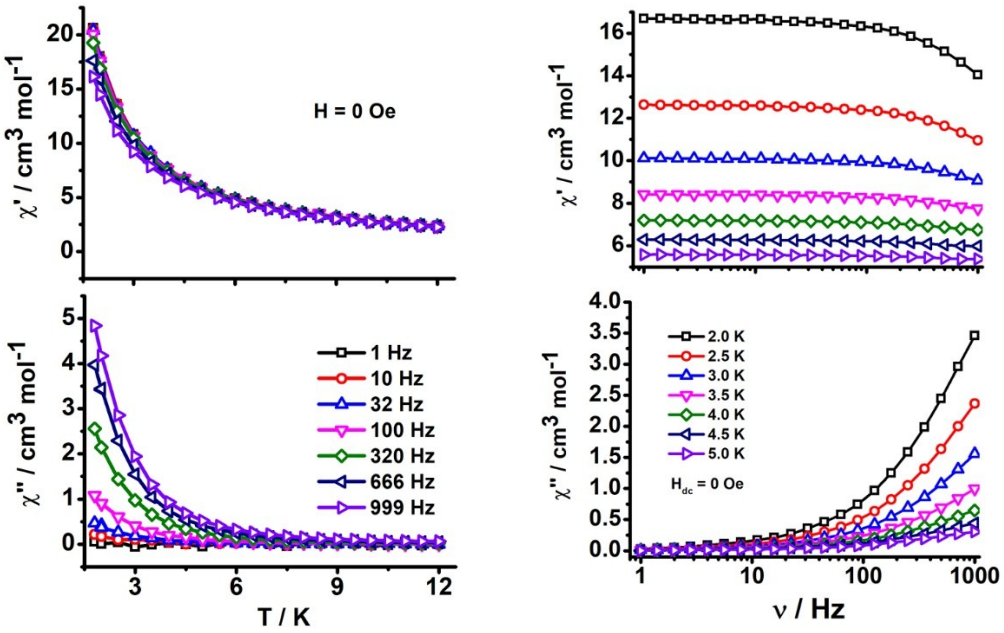

Fig. S8 Temperature- and frequency- dependent in-phase (χ') and out-of-phase (χ'') ac susceptibilities data for complex **1** under H_{dc} = 0 Oe.

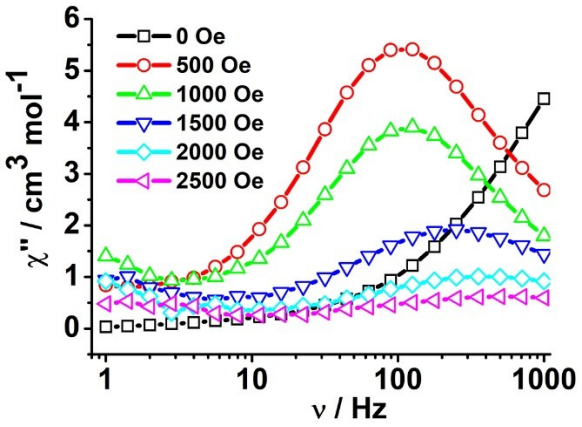

Fig. S9 Frequency-dependence out-of-phase (χ'') ac susceptibility for complex **1** at 2.5 K under different external fields.

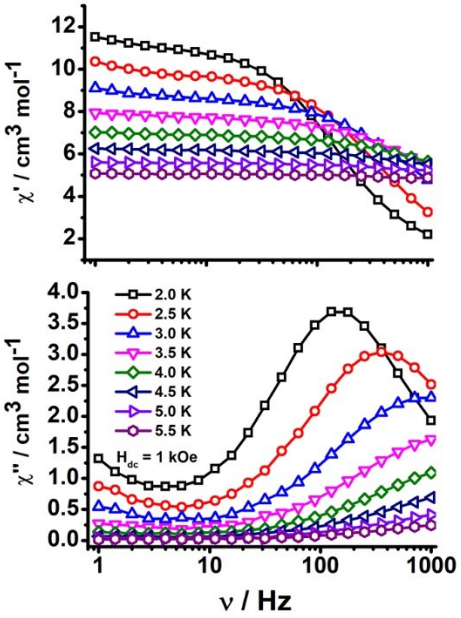

Fig. S10 Frequency-dependent in-phase (χ') and out-of-phase (χ'') ac susceptibilities of complex **1** from 2.0 to 5.5 K under H_{dc} = 1 kOe.

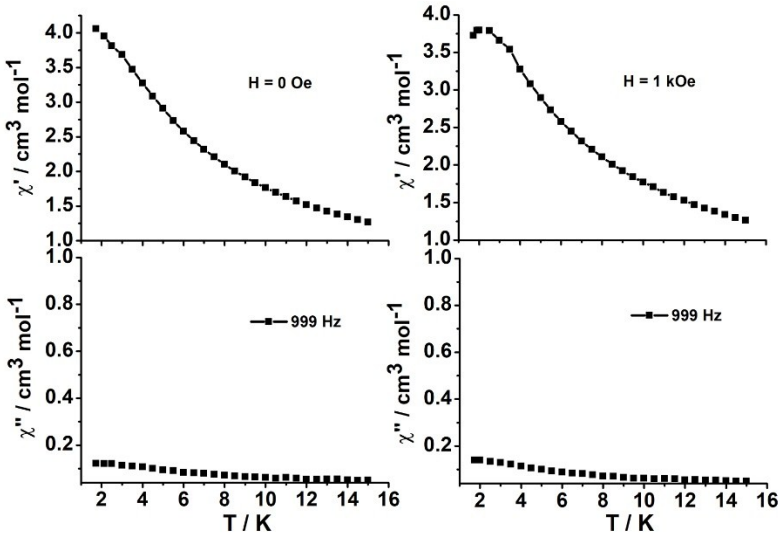

Fig. S11 Temperature-dependent in-phase (χ′) and out-of-phase (χ′′) ac susceptibilities of complex **2** at the frequency of 999 Hz under H_{dc} = 0 Oe (left) and H_{dc} = 1 kOe (right).

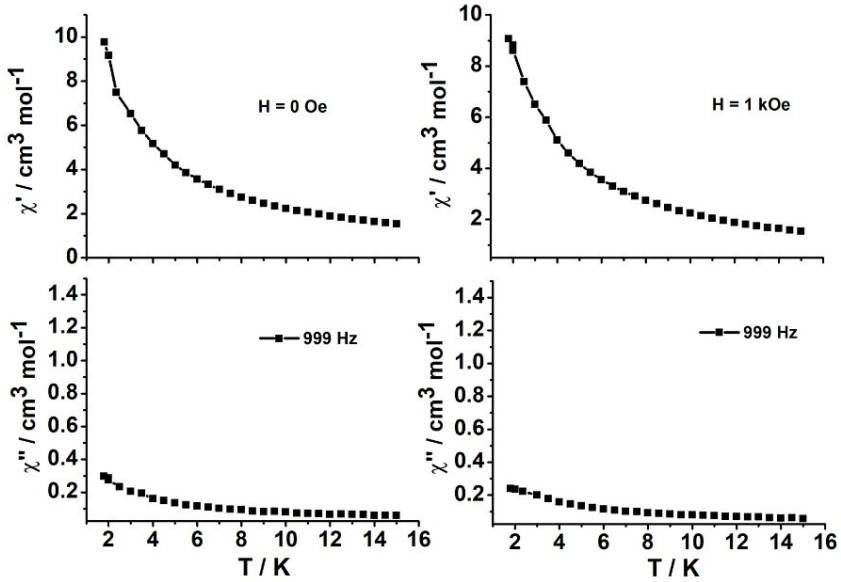

Fig. S12 Temperature-dependent in-phase (χ′) and out-of-phase (χ′′) ac susceptibilities of complex **3** at the frequency of 999 Hz under H_{dc} = 0 Oe (left) and H_{dc} = 1 kOe (right).

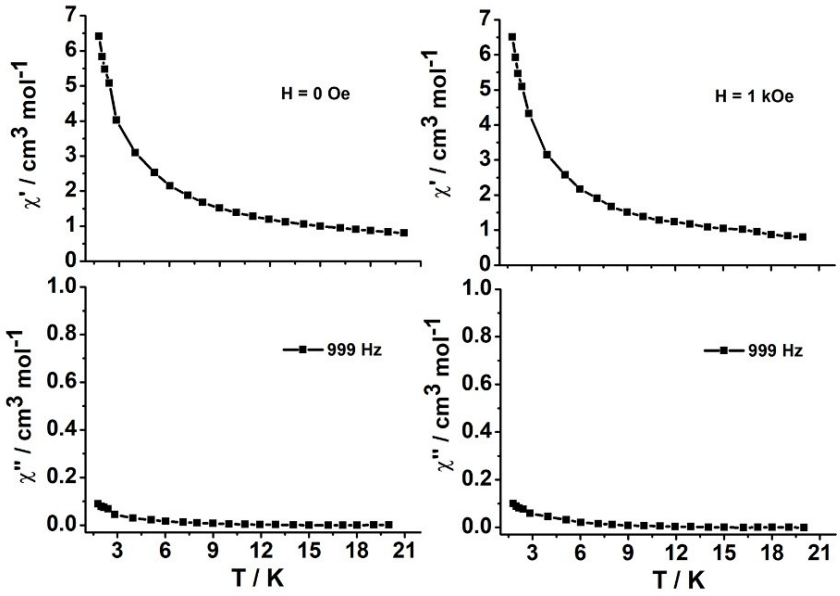

Fig. S13 Temperature-dependent in-phase (χ′) and out-of-phase (χ′′) ac susceptibilities of complex **4** at the frequency of 999 Hz under H_{dc} = 0 Oe (left) and H_{dc} = 1 kOe (right).

Table S1 Selected bond lengths (Å) and angles (°) for complexes **2**–**5**.

	2	**3**	**4**	**5**
Ln(1)-O(1)	2.335(2)	2.321(3)	2.315(3)	2.358(3)
Ln(1)-O(2)	2.330(2)	2.319(3)	2.312(3)	2.357(3)
Ln(1)-O(3)	2.333(2)	2.321(3)	2.311(3)	2.357(3)
Ln(1)-O(4)	2.341(2)	2.340(3)	2.326(3)	2.373(3)
Ln(1)-O(5)	2.337(2)	2.312(3)	2.297(3)	2.342(3)
Ln(1)-O(1)#1[b]	2.370(2)	2.357(3)	2.353(3)	2.379(3)
Ln(1)-Ln(1)#1[b]	3.895(4)	3.886(7)	3.875(7)	3.937(7)
Ln(1)-N(1)	2.601(3)	2.590(4)	2.581(4)	2.627(3)
Ln(1)-N(2)	2.560(3)	2.540(4)	2.545(4)	2.571(4)
O(2)-Ln(1)-O(3)	72.90(8)	73.10(11)	73.52(13)	72.40(12)
O(4)-Ln(1)-O(5)	73.36(7)	73.43(10)	73.51(12)	72.55(10)
O(3)-Ln(1)-O(4)	72.01(8)	72.21(10)	72.15(11)	72.69(10)
O(2)-Ln(1)-O(5)	73.82(8)	73.47(10)	73.30(11)	74.27(10)
N(1)-Ln(1)-N(2)	75.52(9)	75.37(12)	75.48(13)	75.09(12)
O(1)-Ln(1)-O(1)#1[b]	68.23(8)	67.67(11)	67.74(12)	67.56(11)
O(1)-Ln(1)-N(1)	70.80(8)	71.02(10)	71.34(11)	69.96(10)
Ln(1)-O(1)-Ln(1)#1[b]	111.77(8)	112.33(11)	112.25(12)	112.44(11)
O(1)-Ln(1)-Ln(1)#1[b]	34.40(5)	34.13(7)	34.19(8)	33.95(7)

[b] Symmetry transformations used to generate equivalent atoms: #1 -x, -y, -z.

Table S2 Summary of structural parameters for complexes **1**–**5**.

	1	**2**	**3**	**4**	**5**
Average Ln-N bond length (Å)	2.575	2.581	2.565	2.563	2.599
Average Ln-O bond length (Å)	2.329	2.339	2.326	2.316	2.359
Ln1 to O2-O3-O4-O5 plane center distance (Å)	1.257(5)	1.263(7)	1.255(5)	1.247(6)	1.276(7)
Ln1 to N1-N2-O1-O1A plane center distance (Å)	1.388(7)	1.386(6)	1.376(6)	1.366(7)	1.418(6)
Dihedral angle between O2-O3-O4-O5 and N1-N2-O1-O1A planes (°)	1.71(9)	1.92(9)	1.89(10)	1.62(9)	1.85(10)
Shortest intermolecular $Ln^{3+}\cdots Ln^{3+}$ distance (Å)	8.593(3)	8.497(5)	8.603(5)	8.606(3)	8.636(3)
Intramolecular $Ln^{3+}\cdots Ln^{3+}$ distance (Å)	3.886(5)	3.895(4)	3.886(7)	3.875(7)	3.937(7)

Table S3 Parameters obtained by continuous shape measurement (CShM) method for study of central Ln(III) coordination sphere of complexes **1**–**5**. (The S values indicate the proximity to the selected ideal polyhedron, S = 0 corresponds to the non-distorted polyhedron).

	1-S_{Dy}	**2-S_{Tb}**	**3-S_{Ho}**	**4-S_{Er}**	**5-S_{Gd}**
Cube (CU, O_h)	9.711	9.640	9.681	9.790	9.445
Square antiprism (SAP, D_{4d})	0.510	0.476	0.482	0.461	0.551
Triangular dodecahedron (TDD, D_{2d})	2.316	2.347	2.316	2.328	2.239
Biaugmented trigonal prism (BTPR, C_{2v})	2.142	2.190	2.130	2.072	2.273

Table S4 Relaxation fitting parameters of the Cole-Cole plots based on the extended Debye model for complex **1** under H_{dc} = 1 kOe in the temperature range of 2.0–5.5 K.

T / K	χ_S / cm^3 mol^{-1}	χ_T / cm^3 mol^{-1}	ln(τ_1 / s)	α_1	ln(τ_2 / s)	α_2	β
2.0	1.207	15.527	−6.890	0.19	−0.624	0.08	0.31
2.5	1.017	11.539	−7.743	0.23	−1.499	0.01	0.15
3.0	1.408	10.842	−8.542	0.28	−1.545	0.33	0.35
3.5	1.937	8.346	−9.176	0.33	−1.485	0.18	0.08
4.0	2.335	7.192	−9.794	0.35	−1.619	0.03	0.05
4.5	2.274	6.301	−11.151	0.41	−2.013	0.170.	0.02
5.0	2.557	5.631	−12.792	0.43	−2.071	0.33	0.01
5.5	2.483	5.543	−14.557	0.45	−2.152	0.30	0.05

Computational details

Binuclear complex **1** has one inversion center, thus only one type of Dy^{III} fragment was calculated. CASSCF calculations on individual Dy^{III} fragment of the model structure extracted from the compound on the basis of single-crystal X-ray determined geometry have been carried out with MOLCAS 8.2 program package. Individual Dy^{III} fragment was calculated keeping the experimentally determined structure of the corresponding compound while replacing the neighboring Dy^{III} ion by diamagnetic Lu^{III}.

The basis sets for all atoms are atomic natural orbitals from the MOLCAS ANO-RCC library: ANO-RCC-VTZP for Dy^{III} ion; VTZ for close O and N; ANO-RCC-VTZP VDZ for distant atoms. The calculations employed the second order Douglas-Kroll-Hess Hamiltonian, where scalar relativistic contractions were taken into account in the basis set and the spin-orbit couplings were handled separately in the restricted active space state interaction (RASSI-SO) procedure. For individual Dy^{III} fragment, active electrons in 7 active spaces include all *f* electrons (CAS(9 in 7)) in the CASSCF calculation. To exclude all the doubts, we calculated all the roots in the active space. We have mixed the maximum number of spin-free state which was possible with our hardware (all from 21 sextets, 128 from 224 quadruplets, 130 from 490 doublets). Single_Aniso program was used to obtain the ***g*** tensors, energy levels, magnetic axes, *et al.,* based on the above CASSCF/RASSI calculations.

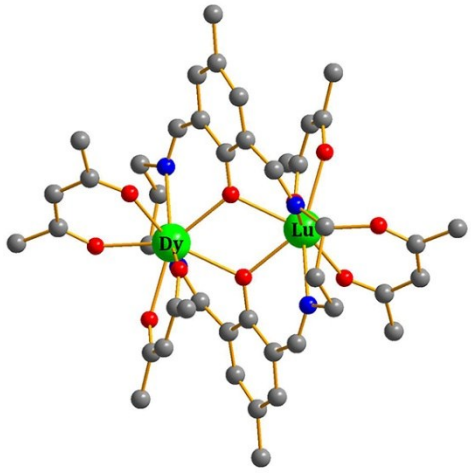

Fig. S14 Calculated model structure of individual Dy^{III} fragment of complex **1** (H atoms are omitted).

Table S5 Calculated energy levels (cm^{-1}), $\boldsymbol{g}$ (g_x, g_y, g_z) tensors and m_J values of the lowest eight Kramers doublets (KDs) of individual Dy^{III} fragment of complex **1**.

KDs	E/cm^{-1}	$\boldsymbol{g}$	m_J
1	0.0	0.026 0.059 18.738	±15/2
2	68.6	0.263 0.317 16.089	±9/2
3	117.5	0.093 0.562 12.519	±11/2
4	163.8	2.044 3.449 8.646	±5/2
5	203.8	4.036 5.912 9.736	±3/2
6	250.0	0.780 1.127 17.557	±7/2
7	298.7	0.092 0.192 19.288	±1/2
8	372.9	0.092 0.192 19.288	±13/2

Table S6 Wave functions with definite projection of the total moment | m_J > for the lowest two Kramers doublets (KDs) of individual Dy^{III} fragment for complex **1**.

E/cm^{-1}	wave functions
0.0	83%|±15/2>+10%|±11/2>
68.6	15%|±13/2>+25%|±9/2>+18%|±7/2>+16%|±5/2>+13%|±3/2>+10%|±1/2>

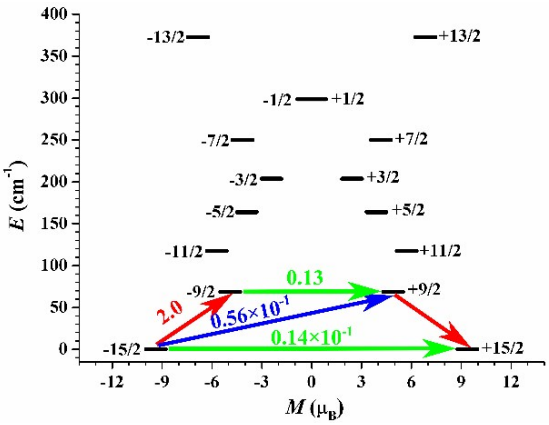

Fig. S15 The magnetization blocking barriers in individual Dy^{III} fragment of complex **1**. The thick black lines represent the Kramers doublets as a function of their magnetic moment along the magnetic axis. The green lines correspond to diagonal quantum tunneling of magnetization (QTM); the blue line represent off-diagonal relaxation process. The numbers at each arrow stand for the mean absolute value of the corresponding matrix element of transition magnetic moment.

To fit the exchange interaction in complex **1**, we took two steps to obtain them. Firstly, we calculated one Dy^{III} fragment using CASSCF to obtain the corresponding magnetic properties. Then, the exchange interaction between the magnetic centers is considered within the Lines model, while the account of the dipole-dipole magnetic coupling is treated exactly. The Lines model is effective and has been successfully used widely in the research field of *f*-elements single-molecule magnets.

For complex **1**, there is only one type of *J*.

The exchange Ising Hamiltonian is:

$$\hat{H}_{exch} = -J_{total}\,\tilde{S}_{Dy1}\,\tilde{S}_{Dy2}$$

The J_{total} is the parameter of the total magnetic interaction ($J_{total} = J_{diploar} + J_{exchange}$) between magnetic center ions. The $\tilde{S}_{Dy}$ = ±1/2 are the ground pseudospin on the Dy^{III} sites. The dipolar magnetic coupling can be calculated exactly, while the exchange coupling constants were fitted through comparison of the computed and measured magnetic susceptibility using the Poly_Aniso program.

Table S7. Exchange energies (cm^{-1}) and main values of the g_z for the lowest two exchange doublets of complex **1**.

	E/cm^{-1}	g_z
1	0.0	37.467
2	1.2	0.000

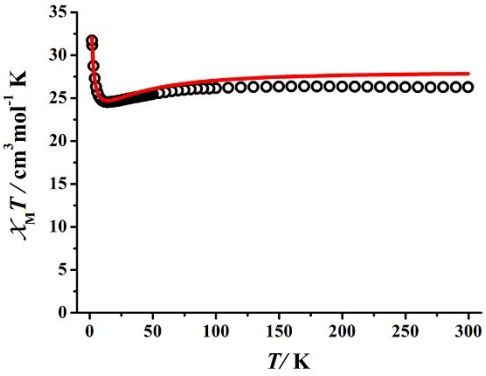

Fig. S16 Calculated (red solid line) and experimental (circle dot) data of magnetic susceptibilities of complex **1**. The intermolecular interactions zJ' of **1** was fitted to 0.00 cm^{-1}.